

RESEARCH

Open Access



Aromatase reduces sperm motility by down-regulating the expression of proteins related to ATP synthesis in seminal plasma extracellular vesicles

Xuliang Luo¹, Yan Guo¹, Xuelian Li¹, Zi Mei¹, Haobo Zhou¹, Ping Qiu¹, Haoxin Wang¹, Yan Chen¹ and Yanzhang Gong^{1*}

Abstract

Background Aromatase, encoded by *Cyp19a1*, is the rate limiting enzyme in biosynthesis of estrogens, and excessive aromatase can reduce the semen quality in roosters. Seminal plasma extracellular vesicles (SPEV) are nanoscale vesicles that carry and transmit signaling molecules, thereby affecting semen quality. Currently it is still unclear whether SPEV are involved in the process of that aromatase affects the quality semen in chicken. To clarify this issue, lentivirus carrying *Cyp19a1* (LV-CYP19A1) for over-expression of aromatase was constructed and injected to testis of 35-week-old roosters. Semen quality and seminal plasma hormone were measured, and SPEV were also extracted and proteome sequencing was performed after treatment of LV-CYP19A1.

Results The results indicated that semen volume, fertility, sperm motility, testosterone (T) levels were significantly decreased, and estradiol (E₂) levels were significantly increased in LV-CYP19A1 group than those in control group ($P < 0.05$). Through proteomic analysis of SPEV, we identified 966 differentially expressed proteins (DEPs) in the comparison of LV-CYP19A1 group and control group. Gene Ontology (GO) and Kyoto Encyclopedia of Genes and Genomes (KEGG) items of DEPs are mainly enriched in ATP synthesis coupled electron transport, flagellated sperm motility, regulation of steroid biosynthetic process, and PI3K-Akt signaling pathway. Furthermore, 8 proteins including ENO4, APOB, SDHA, SDHB, UQCRC1, VIN, PITGB3 and FXN were identified as key proteins in SPEV involving in the process of aromatase regulated rooster semen quality.

Conclusions Our results reveal that aromatase can down-regulate the protein expression related to regulation of ATP synthesis and metabolism, and sperm motility in SPEV, thereby reducing semen quality in roosters.

Keywords Roosters, Aromatase, *Cyp19a1*, Extracellular vesicles, Sperm motility

Background

With the age of roosters more than 45 weeks, the estradiol (E₂) levels increase and testosterone (T) levels decrease, resulting in a decline in semen quality, and subsequently affecting the reproductive performance [1–4]. Aromatase is one of the cytochromes P450 enzyme series, encoded by *Cyp19a1*, which can catalyze the formation of estrogen from androgens, and is a key

*Correspondence:

Yanzhang Gong
poultry@mail.hzau.edu.cn

¹ Key Laboratory of Agricultural Animal Genetics, Breeding and Reproduction of Ministry of Education, College of Animal Science and Technology and College of Veterinary Medicine, Huazhong Agricultural University, 430070 Wuhan, People's Republic of China



rate limiting enzyme in estrogen biosynthesis [5–7]. The decline of semen quality in aged roosters is related to aromatase. Over-expression of aromatase will increase the serum E_2 levels and decrease T levels, thereby affecting sperm motility and reproductive performance [8, 9]. It was found that turkeys with high sperm motility exhibited relatively lower aromatase expression levels and higher T levels than those with low sperm motility [10]. In chicken, aromatase inhibitors were used to reduce aromatase activity, increase testicular weight and plasma T levels, and improve semen density and sperm motility, thus improving the reproductive performance of aged roosters [11, 12]. However, how the aromatase affects semen quality is still unclear.

Extracellular vesicles (EVs) are natural nanoparticles containing bioactive molecules, which are widely present in various body fluids, such as semen, plasma, urine, and milk, and are an important pathway for intercellular communication [13–15]. EVs with a diameter range of 30 nm to 250 nm can be secreted by various cell and contain various cellular products, including DNA, RNA, proteins and lipids [16, 17]. In mammals, EVs are generally associated with most physiological processes [18]. Semen EVs have been considered to promote of sperm motility and regulate capacitation process [19, 20]. These functions are based on their ability to transport biomolecules to the sperms [21]. Compared with asthenospermic patients, the cysteine-rich secreted protein-1, which has the function of regulating sperm motility, was significantly up-regulated in the SPEV of normal males, while the inhibitory protein glycodeilin was significantly down-regulated [20]. Most proteins related to the epididymosomes and prostasomes are transferred to the subcellular or membrane domains of sperm during epididymal transport, and are involved in the acquisition of fertilization ability, regulation of sperm motility and capacitation [22]. In avian, Luo et al. (2022) screened multiple proteins related to sperm maturation and function through proteomic sequencing and found that those proteins involved in endopeptidase inhibitor activity and calcium binding may support sperm survival [16]. Cordeiro L. (2021) reported that SPEV appeared more abundant in fertile roosters than in subfertility roosters, and adding SPEV from fertile roosters to the semen of subfertile roosters could improve their sperm motility [23].

At present, the effects of both aromatase and SPEV on sperm motility have been studied separately, and whether aromatase can regulate sperm motility through SPEV has not been reported. In this study, we injected lentivirus carrying *Cyp19a1* for over-expression of aromatase into the testis of 35 -week-old roosters and measured semen quality, serum and seminal plasma T and E_2 levels. Subsequently, we isolated SPEV and performed proteomic

sequencing, aiming to reveal the molecular mechanisms of aromatase mediated SPEV regulation of rooster semen quality.

Methods

Construction of lentiviruses over-expressing *cyp19a1*

The PLVX-EGFP-Puro-CYP19A1 shuttle plasmid was obtained by inserting the coding sequence of *Cyp19a1* on the PLVX-EGFP-Puro vector (Fig. 1A). PLVX-EGFP-Puro-CYP19A1 plasmid, backbone plasmid and transfection reagent Lip2000 were added to HEK293T cells with good growth conditions, and incubated in an incubator at 37°C with 5% CO_2 for 8 h. Subsequently the culture medium was changed and the culture was continued for 48 h. To obtain the PLVX-EGFP-Puro-CYP19A1, the cell supernatant was collected, centrifuged at 3500 rpm for 10 min, and the precipitate was discarded. The supernatant was filtered with a 0.22 μ m filter membrane, and then centrifuged at 30,000 rpm for 2 h. the supernatant was discarded, and the precipitate was resuspended with 100 μ L of precooled PBS solution. Finally, the virus titer was detected and stored at $-80^\circ C$. Primers are listed in Table S1.

Experimental animals

Seventy 35-week-old sexually mature Gushi roosters were purchased, and their body weight and semen quality were tested. Ten roosters with similar body weight and semen quality were selected and raised in the experimental chicken farm of Huazhong Agricultural University (Wuhan, China), and divided into control group (Control) and lentivirus treatment group (LV-CYP19A1), with five chickens in each group. The control group and LV-CYP19A1 treated group roosters were anesthetized by injecting pentobarbital sodium into the wing vein, the dose was converted according to the proportion of 40 mg/kg of the body weight of each rooster. Then an opening about 1 cm was made from the spine between the last and penultimate ribs of the rooster using a surgical method. The left testis of the roosters in the control group and the LV-CYP19A1 group were injected with 4 μ L empty lentivirus and lentivirus carrying *Cyp19a1* (LV-CYP19A1) with a lentivirus titer of 3.28×10^6 pfu/mL by microinjector (Fig. 1B). After the fixed-point injection, the wound was sutured with absorbable suture and disinfected with 75% medical-grade alcohol. The experimental birds were kept in individual cages, given standard diet and ad libitum drinking water, and their health status was monitored. From 20 days later, the semen quality of experimental birds was measured once a week until day 55, and significant differences in semen quality between the control group and LV-CYP19A1 group were detected. Subsequently, semen quality and hormone determination

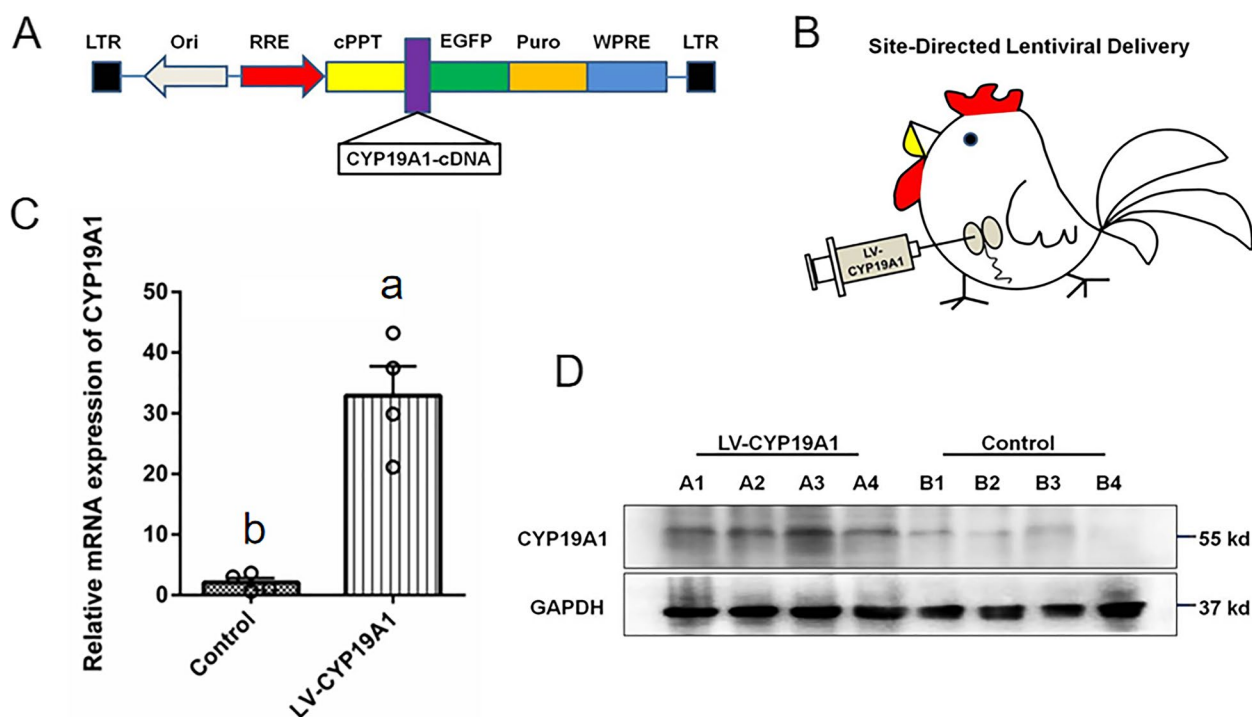


Fig. 1 *Cyp19a1* expression level detection and semen quality assessment of control group and LV-CYP19A1 group roosters. **A** Construction of *Cyp19a1* over-expression vector. **B** Diagram of injection of lentivirus carrying *Cyp19a1* over-expression vector into rooster testis. **C** qRT-PCR results of *Cyp19a1* in control group and LV-CYP19A1 group. **D** WB results of *Cyp19a1* in control group and LV-CYP19A1 group. ^{a-b} Different letters within the same row show significant differences among the groups ($P < 0.05$)

were conducted every other day, and artificial insemination was also performed to test the fertilization rate.

Semen quality and fertility evaluation

The semen samples of control and the LV-CYP19A1 treated roosters were collected by trained professionals. Semen volume was measured with pipettes of different range of sizes. Semen parameters were determined by Computer-Assisted Semen Analysis (CASA, Minitube, Germany) after diluting (at 1:80) the semen with normal saline. Each indicator was repeated three times. The fresh semen of the roosters in the control group and the LV-CYP19A1 group were collected for artificial insemination, and eggs were collected for artificial incubation and the fertilization rate of eggs was counted.

Detection of T and E₂ in serum and seminal plasma

Blood and semen of roosters in the control and LV-CYP19A1 groups were collected, respectively. Serum and seminal plasma were separated at 2500 rpm/min after kept at room temperature for 60 min. According to enzyme linked immunosorbent assay (ELISA, ThermoFisher, USA) instructions of E₂ and T, 10 μ L of the serum and seminal plasma and 40 μ L of the sample diluent were added to the sample wells. Then 100 μ L of

HRP-Conjugate reagent was added, sealed and incubated at 37°C for 60 min. The closure plate membrane and liquid were discarded, and the sample wells were washed five times with washing solution. Then the chromogen solution was added and evade the light preservation at 37°C for 15 min. Finally, the absorbance of the sample wells after adding stop solution was measured within 15 min using an ELISA detector (Tecan, Switzerland).

Isolation and preparation of SPEV samples

SPEV samples from the control and LV-CYP19A1 groups were separately processed by the ultrahigh-speed differential centrifugation [24]. The 1 mL semen sample was centrifuged at 1000 g, 4°C for 10 min after diluting (at 1:40) with phosphate buffer saline, and then residual cells and debris were removed by centrifugation at 12,000 g, 4°C for 30 min. The 0.45 μ m and 0.22 μ m filters were used to filter the larger vesicles in the supernatant, and then ultracentrifugation was performed twice at 100,000 g, 4°C for 90 min. Finally, the SPEV samples precipitated from the control group and LV-CYP19A1 group were resuspended in PBS and stored at -80°C. The Beckman Optima XE-90 ultracentrifuge with an SW-32Ti rotor (Beckman Coulter, USA) were used for ultrahigh-speed differential centrifugation.

SPEV morphology was determined by transmission electron microscopy

SPEV sample was dropped onto a copper mesh with a pore size of 2 nm and kept at room temperature for 2 min. Following that the membrane surface of the mesh was put on the SPEV droplet, suspended it for 10 min, and dried with filter paper. Then negative staining was performed with 3% phosphotungstic acid solution for 5 min and samples were air-dried. Finally, SPEV samples were observed by H-7650 100 kV analytical transmission electron microscope (TEM, Hitachi, Japan).

SPEV size was determined by nanoparticle tracking analysis

Nanoparticle tracking analysis (NTA, particle metrix, Germany) was used to detect particle size of SPEV samples. The sample wells were cleaned with PBS and filtered molecular water (Biological Industries, Israel). SPEV samples were diluted with filtered molecular water at 1:40,000. The instrument was calibrated with polystyrene microspheres (110 nm). Blank pool added with filtered molecular-grade water was used as a negative control. Laser was used to irradiate the particles in the suspension, and the scattered light was captured by the video camera to track the change of particle position and determine the diffusion of particles. The particle diameter was calculated according to the diffusion coefficient, and then the NTA software ZetaView was used to generate the particle size distribution and counting. The procedure was repeated three times for each sample.

SPEV marker proteins were detected by western blot

Identification of marker proteins in SPEV samples by western blot (WB). SPEV suspension (1:1 v/v) was mixed with radioimmunoprecipitation assay lysis buffer (RAPI, Vazyme, China) and phenylmethanesulfonyl fluoride (PMSE, Vazyme, China), and after incubation at 4°C for 15 min, the supernatant was collected to obtain SPEV protein after centrifugation at 12,000 rpm for 15 min. The concentration of SPEV protein was measured by BCA detection kit (Biosharp, China). The SPEV protein was mixed with protein loaded dye (Biosharp, China), denatured at 98°C, and subjected to 10% SDS polyacrylamide gel electrophoresis (Biosharp, China) at 120 V for 80 min. The isolated gel protein was transferred to polyvinylidene fluoride membrane (PVDF, Vazyme, China) at 200 mA for 90 min, and blocked with 5% bovine serum albumin (BSA, MedChemexpress, USA) at room temperature for 60 min. The PVDF membranes were incubated with primary antibodies CYP19A1 (BIO-RAD, MCA2077S), CD9 (abclonal, A19027), TSG101 (abcam, ab133586),

and ALIX (abclonal, A2215) proteins at 4°C overnight. After cleaning, PVDF membrane was incubated with secondary antibody at room temperature for 60 min, and detected by chemiluminescent kit (Abbkine, USA).

Tandem mass tag proteomic analysis of SPEV

The SPEV samples of the control group and LV-CYP19A1 group roosters were mixed with 1% protease inhibitor, sonicated to lyse the SPEV samples, centrifuged at 12,000 g, 4°C for 10 min, and the supernatant was separated. The protein concentration was determined by BCA assay kit. After lysing the protein samples with lysis buffer, acetone was added and precipitated at -20°C for 120 min, centrifuge at 4500 g for 5 min, discard the supernatant, air-dry the precipitate, and incubate overnight with trypsin. Then add dithiothreitol (DTT) and iodoacetamide (IAA), and incubate at room temperature in the dark for 15 min. The peptide segments were classified by high pH reverse phase HPLC using an Agilent 300extend C18 chromatographic column. After separation by an ultra-high performance liquid chromatography system, the peptide was injected into an NSI ion source for ionization, and then analyzed by Thermo Scientific TMQ active hf-x mass spectrometry. The raw data was retrieved using Proteome Discoverer (V.2.4.1.15) [25], with the reference database being G Gallus reference proteome (Blast/Gallus/Gallus/9031/PR/2020_0727.fasta). Proteins with an adjusted $P < 0.05$ and Fold Change > 1.5 were designated as differentially expressed proteins (DEPs). PCA analysis was performed using the R (V.4.1.2) [26], and visualized the PCA results by R package ggplot2 (V.3.5.0) [27]. DEPs were annotated using GO and KEGG (<http://bioinfo.org/kobas>) [28]. PPI network analysis was conducted through the STRING (V.11.0, <https://cn.string-db.org/>) [29], and the network was presented using Cytoscape (V3.8.1, <http://www.cytoscape.org/>) software [30].

Quantitative Real-Time PCR validation

The total RNA of SPEV samples was extracted by the trizol method, and then the RNA was reverse-transcribed to cDNA using a reverse transcription kit. qRT-PCR was performed in ABI Quant Studio system (Life Technics, USA), and SYBR Green fluorescent dye was used as a molecular probe for qRT-PCR reaction, with reaction conditions were set to 45 cycles of 95°C for 3 min, 95°C for 15 s, 60°C for 15 s, 72°C for 20 s, and 95°C for 5 s. qRT-PCR gene primers are listed in Table S1. Relative gene expression was calculated using the $2^{-\Delta\Delta Ct}$ method.

Statistical analysis

Student's t-test was performed using SPSS 22.0 software to determine differences between groups. Data were

expressed as means \pm SEM, $P < 0.05$ was considered as statistically significant. Graphs were plotted using the GraphPad Prism 8.0.

Table 1 Semen quality parameters of control group and LV-CYP19A1 group roosters

Traits	Control	LV-CYP19A1
Volume (μ L)	450.00 \pm 150.55 ^a	293.40 \pm 175.02 ^b
Fertility (%)	96.74 \pm 1.35 ^a	89.71 \pm 1.30 ^b
Sperm motility (%)	95.12 \pm 4.01 ^a	91.78 \pm 0.87 ^b
VSL (μ m/s)	105.39 \pm 11.03 ^a	81.62 \pm 17.51 ^b
VCL (μ m/s)	255.40 \pm 65.45 ^a	186.26 \pm 24.97 ^b
VAP (μ m/s)	146.17 \pm 14.21 ^a	105.18 \pm 14.98 ^b
ALH (μ m)	2.86 \pm 0.64	1.99 \pm 0.32
LIN (%)	41.26 \pm 1.72	44.00 \pm 9.14
STR (%)	72.10 \pm 1.31	77.20 \pm 6.46
WOB (%)	57.23 \pm 3.22	57.00 \pm 6.89

^{a-b} Different letters within the same row show significant differences between groups ($P < 0.05$). Notes: VSL, straight-line velocity, VCL curvilinear velocity, VAP average path velocity, ALH amplitude of lateral head displacement, LIN linearity (VSL/VCL), STR, straightness (VSL/VAP), WOB wobble (VAP/VCL)

Results

Over-expression of *cyp19a1* reduces the semen quality of roosters

The expression of *Cyp19a1* in testis was detected by qRT-PCR and WB. The results showed that the expression of *Cyp19a1* in the LV-CYP19A1 group was significantly higher than that of control group ($P < 0.05$, Fig. 1C-D). The semen quality and fertility were evaluated by CASA (Table 1). The semen volume, sperm motility, fertility, VCL, VSL and VAP of control group were significantly higher than LV-CYP19A1 group ($P < 0.05$). These results indicated that over-expression of aromatase could reduce the semen quality and reproductive performance of roosters.

Over-expression of *cyp19a1* reduces T hormone levels, and increases E₂ hormone levels in serum and seminal plasma

The serum and seminal plasma hormone levels were measured by ELISA. The results showed that the T levels of serum and seminal plasma in control group was significantly higher ($P < 0.05$, Fig. 2A-B), and the E₂ levels of seminal plasma was significantly lower than of LV-CYP19A1 group ($P < 0.05$, Fig. 2C). Compared with the control group, the serum E₂ levels in LV-CYP19A1 group

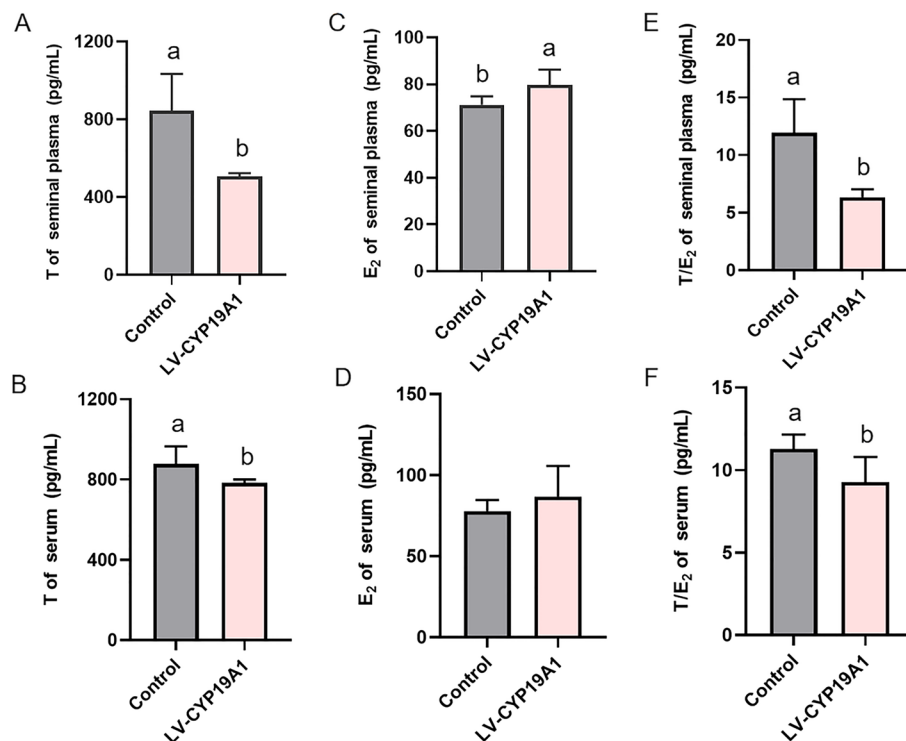


Fig. 2 Serum and seminal plasma hormone levels detection of control group and LV-CYP19A1 group roosters. Seminal plasma T (A), E₂ (C), and T/E₂ (E) levels of control group and LV-CYP19A1 group. Serum T (B), E₂ (D), and T/E₂ (F) levels of control group and LV-CYP19A1 group. ^{a-b} Different letters within the same row show significant differences among the groups

had an upward trend, but it was not significant (Fig. 2D). The T/E_2 of serum and seminal plasma in control group was greater than 10, while in LV-CYP191 group was less than 10. The above results indicated that over-expression of aromatase reduces T levels, and increases E_2 levels in serum and seminal plasma.

Identification and characterization of SPEV

The morphology, particle size and marker proteins of SPEV were characterized by TEM, NTA and WB, respectively. The TEM results showed that SPEV exhibited bilayer membrane structure (Fig. 3A-B). The NTA revealed that the particle size of SPEV in control and LV-CYP19A1 groups ranged from 30 to 250 nm, with a main peak at 170.8 nm and 172.2 nm, respectively (Fig. 3C-D). Marker proteins TSG101, ALIX and CD9 of EVs were detected (Fig. 3E). These results indicated that SPEV were successfully isolated from the control and LV-CYP19A1 groups.

Identification and functional annotation of SPEV DEPs

To investigate the effect of SPEV on the semen quality of rooster after over-expressing *Cyp19a1*, we performed

proteomic sequencing of SPEV. PCA analysis showed that control group and LV-CYP19A1 group were clustered well separately (Fig. 4A). By analyzing proteomic data, the volcanic map results showed that 966 DEPs were identified from SPEV between control group and LV-CYP19A1 group, 303 DEPs were up-regulated and 663 DEPs were down-regulated (Fig. 4B). Heatmap of DEPs were plotted in Fig. 4C. GO and KEGG enrichment analysis was performed on DEPs (Fig. 5A-B). The significantly enriched GO terms were ATP synthesis coupled electron transport, flagellated sperm motility, and regulation of steroid biosynthetic process in biological processes; ATP-dependent microtubule motor activity, cholesterol binding, sterol binding and electron transfer activity in molecular functions; sperm flagellum, cytoplasmic vesicle lumen, and mitochondrial respiratory chain complex III in cellular components. KEGG enrichment analysis showed that the DEPs were mainly enriched in steroid biosynthesis, Cholesterol metabolism, PI3K-AKT signalling pathway, and calcium signalling pathway. These results indicate that over-expression of aromatase is involved in the regulation of ATP biosynthesis and steroid hormone, and may mediate sperm motility.

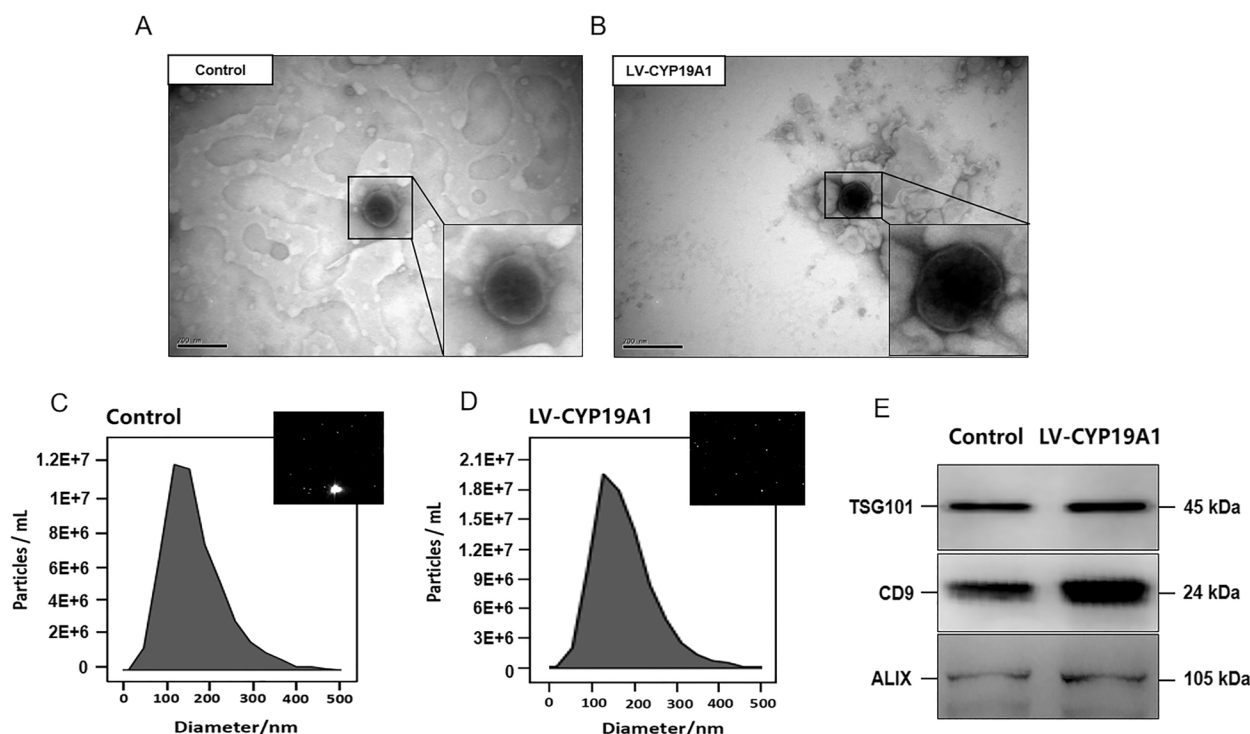


Fig. 3 Morphology, particle size, and marker proteins identification of seminal plasma extracellular vesicles (SPEV). **A-B** Morphological characteristics of SPEV in control group and LV-CYP19A1 group. **C-D** Particle size distribution of SPEV in control group and LV-CYP19A1 group. **E** Western Blot (WB) analysis of the common SPEV marker proteins

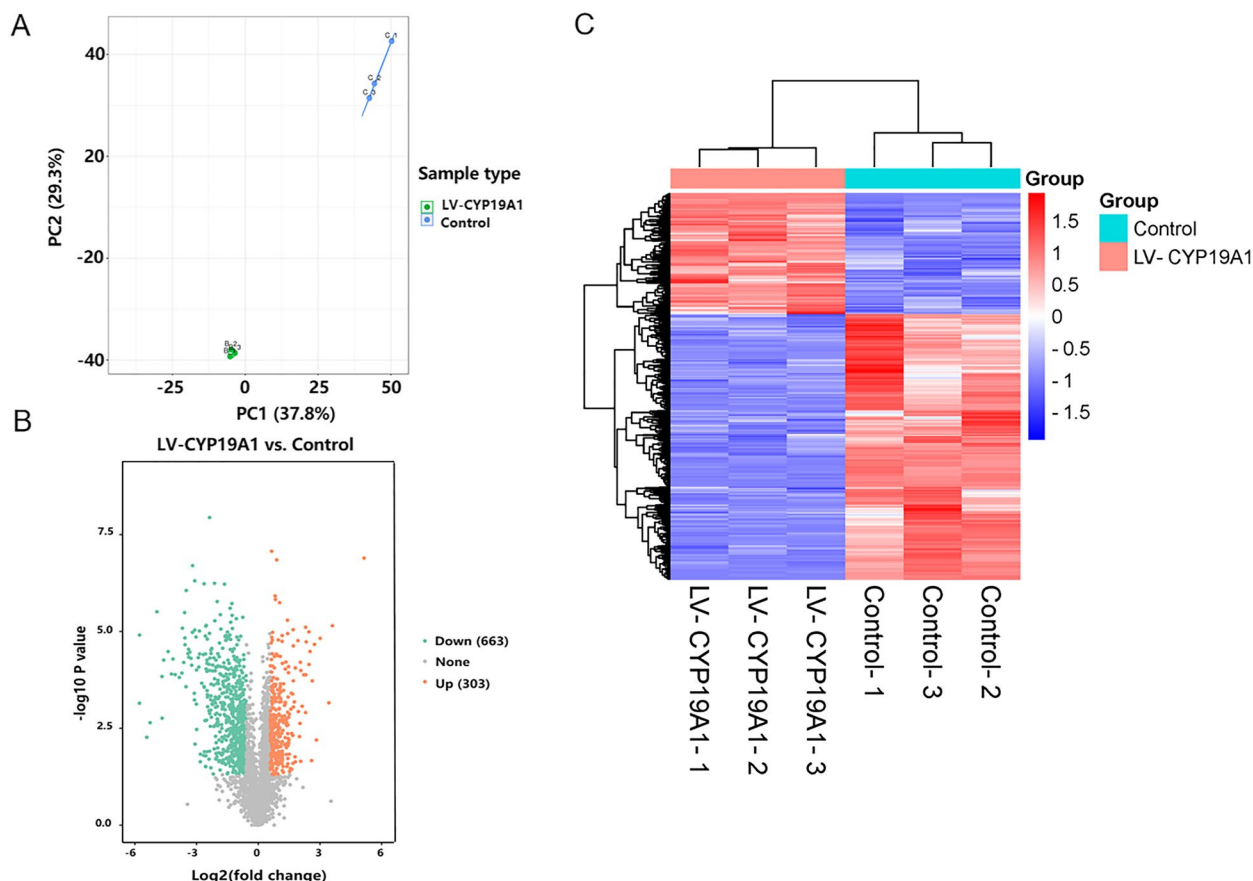


Fig. 4 Identification of differentially expressed proteins (DEPs) between control group and LV-CYP19A1 group. **A** Principal component analysis (PCA) of DEPs between control group and LV-CYP19A1 group. **B** Volcanic maps of DEPs between control group and LV-CYP19A1 group. **C** Heatmap of DEPs between control group and LV-CYP19A1 group

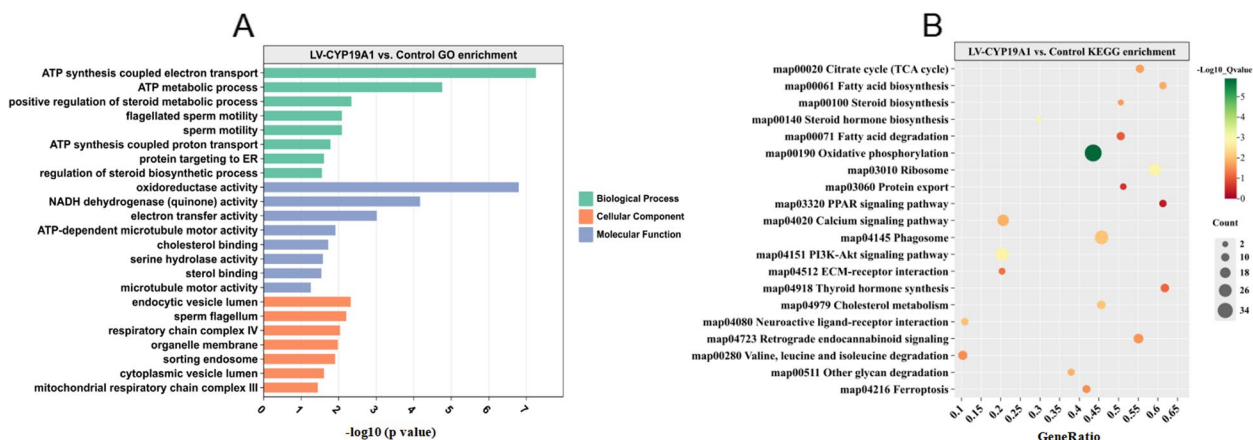


Fig. 5 GO and KEGG analysis of differentially expressed proteins (DEPs) between control group and LV-CYP19A1 group. **A** GO analysis of DEPs between control group and LV-CYP19A1 group. **B** KEGG analysis of DEPs between control group and LV-CYP19A1 group

PPI analysis of DEPs involved in key pathways and biological processes

To study the interaction between the proteins, we

analyzed the PPI network of DEPs which were enriched in key pathways and biological processes. The protein-biological process networks consisted of 7 key biological

processes and 68 DEPs (Fig. 6A). It showed that ENO4, APOB and FXN were involved in several key biological processes. ENO4 was enriched in ATP metabolic process, sperm motility, and flagellated sperm motility; APOB was enriched in regulation of steroid biosynthetic process, sperm motility, and flagellated sperm motility; FXN was enriched in ATP metabolic process, regulation of steroid biosynthetic process, and positive regulation of steroid metabolic process. To investigate the interaction relationship between ENO4, APOB, FXN and other proteins, we further performed PPI analysis of 62 DEPs

involved in key biological processes (Fig. 6B). The results indicated that ENO4, APOB and FXN can interact with 10, 2 and 5 key DEPs, respectively. The key proteins that interact with ENO4 are mainly enriched in ATP synthesis coupled electron transport (SDHA, SDHB, NDUFS8, UQCRC1, FXN), ATP metabolic process (ALDOB, ATP5C1, ATP5A1Z, DLD, AK9), sperm motility (ENO4, SPAG6, TEKT2, TEKT3, GAS8); The key proteins that interact with FXN are enriched in ATP synthesis coupled electron transport (SDHA, SDHB), and ATP metabolic process (UQCRC1, UQCRC2, UQCRFS1). SDHA, SDHB

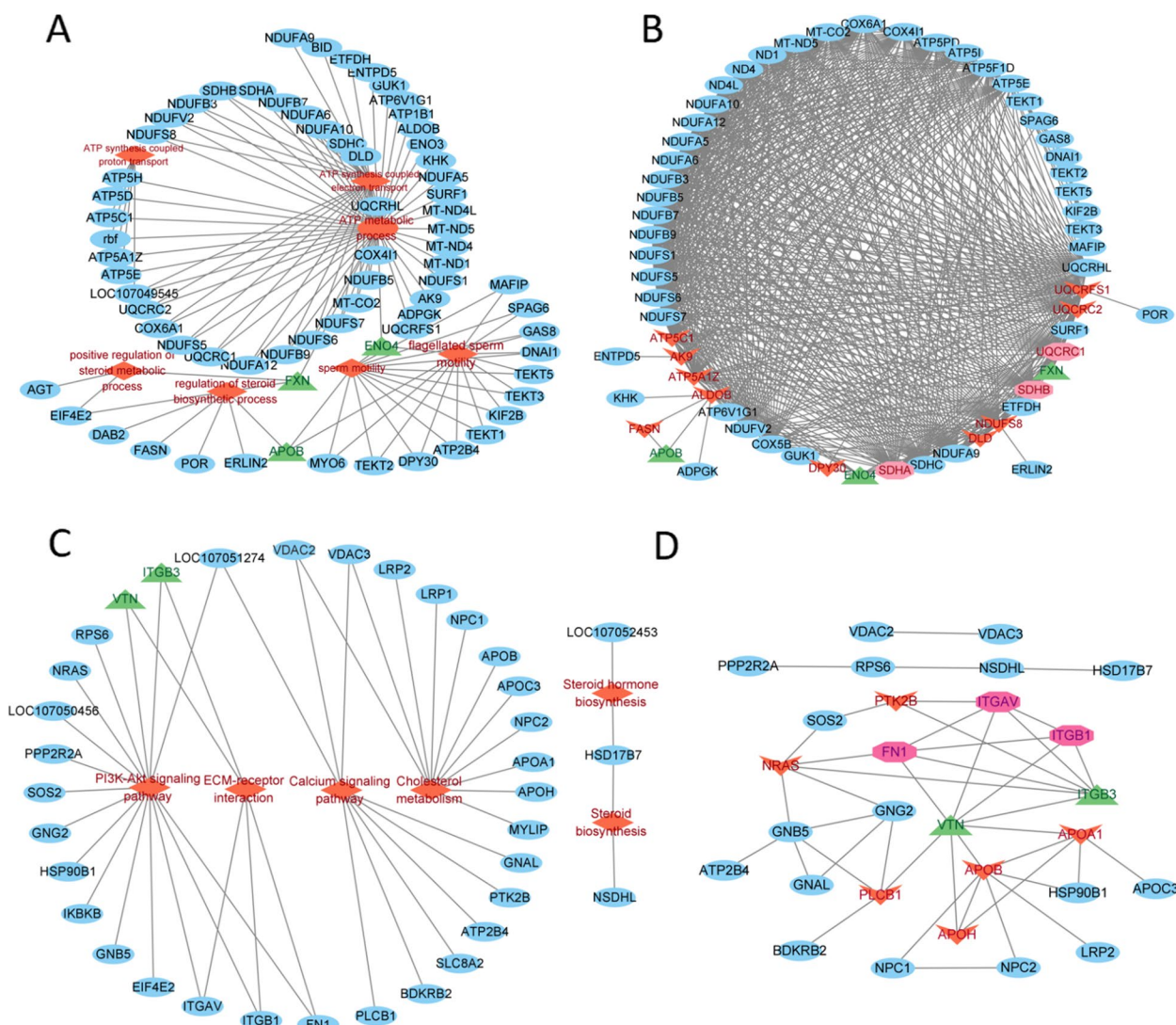


Fig. 6 Key protein-biological process, protein-pathway, and protein-protein interaction (PPI) analysis of differentially expressed proteins (DEPs). **A** Key protein-biological process analysis of DEPs between control group and LV-CYP19A1 group. **B** PPI analysis of DEPs involved in key biological processes between control group and LV-CYP19A1 group. **C** Key protein-pathway analysis of DEPs between control group and LV-CYP19A1 group. **D** PPI analysis of DEPs involved in key pathways between control group and LV-CYP19A1 group. Orange diamonds represent the key pathways and biological processes; Green triangles represent the key proteins; Orange inverted triangles represent proteins that interact with individual key proteins; Pink octagon represent proteins that interact with multiple key proteins

and UQCRC1 can interact with ENO4 and FXN, which may play an important role in regulating sperm motility. The key DEPs related to regulation of steroid metabolic process, ATP metabolic and synthesis process, and sperm motility are shown in Table 2. The protein-pathway networks consisted of 6 key pathways and 36 DEPs (Fig. 6C-D). The results indicated that VIN and ITGB3 were enriched in PI3K-Akt signaling pathway and ECM-receptor interaction, and could interact with multiple DEPs. The key proteins that interact with VIN and ITGB3 are mainly enriched in PI3K-Akt signaling pathway (NRAS) and ECM-receptor interaction (ITGB1, ITGAV, FN1), calcium signaling pathway (PTK2B, PLCB1), and cholesterol metabolism (APOH, APOB, APOA1). The results

suggested that over-expression of aromatase may affect sperm motility by down-regulation of expression proteins involved in ATP synthesis and metabolism in SPEV. ENO4, APOB, FXN, SDHA, SDHB, UQCRC1, VIN and ITGB3 may play the most critical role in these processes.

Discussion

Semen quality is a crucial reproductive trait in poultry production and breeding, and good semen quality is an important foundation for maintaining high fertility [31, 32]. T and E₂ are steroid hormones related to semen quality, and the balance of T and E₂ is essential for maintaining male reproductive functions [33–35]. Aromatase can convert T into E₂, which is one of the key reasons

Table 2 Key differentially expressed proteins related to regulation of steroid metabolic process, ATP metabolic and synthesis process, and sperm motility

Protein name	Protein accession	Protein description	P value	Control vs. LV-CYP19A1
POR	F1P2T2	NADPH-cytochrome P450 reductase	0.019	down
APOA1	P08250	Apolipoprotein A-I	5.88E-07	down
APOB	F1NV02	Apolipoprotein B	5.68E-05	down
FXN	F1P1P5	Frataxin intermediate form	0.025	down
AGT	F1NDH2	Angiotensin 1-10	9.28E-05	down
NPC2	F1N9N4	Epididymal secretory protein E1	0.010	down
ATP5D	A0A1D5NW93	ATP synthase F1 subunit delta	0.025	down
DLD	Q5ZM32	Dihydrolipoyl dehydrogenase	0.047	down
SDHA	F1NPJ4	Succinate dehydrogenase flavoprotein subunit	4.16E-04	down
SDHB	A0A1D5PIF0	Succinate dehydrogenase iron-sulfur subunit	4.70E-04	down
SDHC	A0A3Q2U2Y6	Succinate dehydrogenase cytochrome b560 subunit	8.74E-03	down
NDUFA6	A0A1D5P4B1	NADH dehydrogenase 1 alpha subcomplex subunit 6	0.002	down
NDUFB7	A0A1D5P384	Complex I-B18	0.010	down
UQCRC1	F1NAC6	Ubiquinol-cytochrome c reductase core protein 1	1.01E-04	down
NDUFB9	A0A1D5PNM0	Complex I-B22	0.012	down
COX4I1	Q5ZJV5	Cytochrome c oxidase subunit 4I1	1.77E-04	down
SPAG6	E1C6P7	Sperm associated antigen 6 (predicted)	2.56E-04	down
NDUFS8	A0A1D5PE41	Complex I-23kD	0.005	down
ENO4	A0A3Q3AEZ3	2-phospho-D-glycerate hydro-lyase	0.002	down
ENO3	P07322	Beta-enolase	0.001	down
ATP1B1	P08251	Sodium/potassium-transporting ATPase subunit beta-1	0.001	down
AK9	F1NRW9	Nucleoside-diphosphate kinase	1.07E-04	down
ADPGK	F1NGR5	ADP dependent glucokinase(predicted)	0.001	down
UQCRC1	Q5ZLR5	Cytochrome b-c1 complex subunit Rieske	0.001	down
KIF2B	A0A3Q2UFD1	Kinesin-like protein	8.39E-04	down
TEKT1	A0A3Q2UCQ4	Tektin	2.71E-05	down
TEKT2	E1C1A3	Tektin	3.84E-06	down
TEKT3	E1BZ49	Tektin	2.91E-05	down
GAS8	F1NLA8	Dynein regulatory complex subunit 4	9.99E-04	down
ALDOB	P07341	Fructose-bisphosphate aldolase B	6.44E-04	down
VDAC3	A0A1L1RKA6	Voltage-dependent anion-selective channel protein 3	0.001	down

for the increase of E_2 and the decrease of T [12]. It has been reported that tol2/ transposase was used to generate transgenic males that can over-express aromatase, which can produce high levels of estradiol and mediate the generation of striped feathers of female traits in males [36]. The levels of T increased in testis of turkey with high sperm motility, and aromatase mRNA and protein expression were significantly down-regulated [10]. Our results indicated that over-expression of aromatase can significantly increase E_2 levels and decrease T levels, which subsequently affect semen volume, sperm motility and fertility of roosters. The DEPs of SPEV were significantly enriched in regulation of steroid biosynthetic and metabolism process, and cholesterol metabolism. The proteins FXN, APOB, APOA1, NPC2 and POR related to steroid biosynthesis and cholesterol metabolism were significantly down-regulated. The sequencing results further verified that aromatase reduced the T hormone levels and semen quality of roosters.

Sperm motility is an important indicator of the semen quality, while the supply of ATP is a key factor affecting sperm motility [37]. It has been reported that ATP can improve sperm motility during in vitro fertilization in humans, pigs, and mice [38–40]. ATP content was positively correlated with the sperm straight-line velocity, flagellum beating frequency and swimming velocity [41–44]. Active release of ATP is mediated by ion channels and EVs [45]. Gardella et al. (2002) reported that ATP could mediate EVs secretion through the high mobility group box 1 protein [46]. Subsequent studies showed that ATP produced by the glycolytic pathway was found in EVs with more plausible evidence for the presence of ATP [47]. At present, it is generally believed that EVs can enwrap ATP and deliver it to target cells [48, 49].

The "omics" method is a powerful tool to understand the genetic and molecular mechanisms related to livestock reproduction [50, 51]. In this study, the proteomic sequencing of SPEV indicated that the DEPs were significantly enriched in ATP synthesis coupled electron transport, ATP metabolic process, and flagellated sperm motility. The proteins ENO4, UQCRC1, VDAC3, SDHA, SDHB, GAS8, AK9, DLD, TEKT2, TEKT3, SPAG6 and MYO6 were involved in ATP synthesis and metabolic processes, and sperm motility were significantly down-regulated in LV-CYP19A1 group. We speculated that aromatase may affect sperm flagellar motility by down-regulating the expression of proteins involved in ATP synthesis, thus affecting sperm motility. ENO4 is located in the sperm principal piece and can participate in the glycolysis and ATP synthesis process, providing energy for sperm cells, and is essential for the motility of sperm flagellum, ENO4 gene knockout mice exhibit abnormal sperm morphology and asthenozoospermia [52]. ENO4

gene mutation can lead to male infertility in humans [53]. Mutations in GAS8, a gene encoding a nexin-dynein regulatory complex subunit, could cause primary ciliary dyskinesia and cause non-syndromic male infertility [54]. ENO4 and GAS8 may be key proteins in the regulation of sperm flagellar motility. VDAC3 is a channel protein in the outer membrane of mitochondria that is believed to play an important role in regulating ATP transport and Ca^{2+} homeostasis [55]. VDAC3 is involved in the formation of the acrosome during spermatogenesis, and VDAC3 deficiency can lead to abnormal mitochondrial sheaths and decreased sperm motility [56–58]. SDHA and SDHB are components of the succinate dehydrogenase (SDH) complex, and SDH activity is positively correlated with sperm quality, SDHA mutations can lead to male infertility [59]. An RNA interference-based silencing of SDHB gene significantly down-regulates multiple proteins involved in glycolysis, reduces sperm count, and inhibits testicular development in "*Macrobrachium nipponense*" [60, 61]. Mitochondria are crucial for sperm quality and male fertility, UQCRC1 is involved in mitochondrial function and sperm capacitation. Boar fertility is controlled through systematic changes of mitochondrial protein ATP5F1 and UQCRC1 expression during sperm capacitation [62]. Tetrabromodiphenyl ether injures cell viability and mitochondrial function of mouse spermatocytes by decreasing mitochondrial proteins ATP5B and UQCRC1 [63]. UQCRC1 and VDAC2 have been reported to be highly sensitive biomarkers for predicting diseases mediated bisphenol-A [62]. Tektin proteins were identified as important proteins related to fertility in livestock [64]. In conclusion, we speculate that ENO4 and GAS8 may mainly regulate sperm flagellar motility, while VDAC2, VDAC3, SDHA, SDHB and UQCRC1 are mainly involved in ATP biosynthesis.

KEGG enrichment analysis showed that the DEPs were mainly enriched in PI3K-AKT signalling pathway, ECM-receptor interaction pathways, and calcium signalling pathway. It has been reported that the PI3K/AKT signaling pathways are involved in regulating various male reproduction processes, including modulating the hypothalamus-pituitary gonad axis during spermatogenesis, promoting proliferation and differentiation of spermatogonia and somatic cells, and regulating sperm autophagy and testicular endocrine functions [65, 66]. ECM-receptor interaction signaling pathway promotes the formation of chicken sperm stem cells [67], while calcium signaling pathway is associated with sperm function. In this study, the proteins VIN, ITGB3, ITGB1, ITGAV and FN1 are involved in multiple biological processes, suggesting their important regulatory effects on sperm functions, which needs to be further investigated.

Conclusions

In summary, the results indicate that aromatase can down-regulate the expression of proteins related to ATP synthesis coupled electron transfer, flagellar sperm motility, and steroid biosynthesis and metabolism in SPEV, decreased T levels and increased E₂ levels in serum and seminal plasma, and ultimately reduce the semen quality of roosters. Furthermore, 8 proteins including ENO4, APOB, SDHA, SDHB, UQCRC1, VIN, PITGB3 and FXN in SPEV were identified as key proteins for aromatase to regulate semen quality in roosters. Our findings are further elucidated the molecular mechanism of aromatase in affecting the reproductive ability of roosters, and lay the theory for subsequent research.

Abbreviations

SPEV	Seminal plasma extracellular vesicles
LV-CYP19A1	Lentivirus carrying Cyp19a1 group
T	Testosterone
E2	Estradiol
DEPs	Differentially expressed proteins
GO	Gene Ontology
KEGG	Kyoto Encyclopedia of Genes and Genomes
EVs	Extracellular vesicles
CASA	Computer-Assisted Semen Analysis
ELISA	Enzyme linked immunosorbent assay
TEM	Transmission electron microscope
NTA	Nanoparticle tracking analysis
WB	Western blot
qRT-PCR	Quantitative Real-Time PCR

Supplementary Information

The online version contains supplementary material available at <https://doi.org/10.1186/s12864-025-11500-5>.

Supplementary Material 1: Table S1: Primer sequences for qRT-PCR.

Supplementary Material 2.

Supplementary Material 3.

Acknowledgements

We thank all the co-authors for their contributions to this article.

Authors' contributions

Xuliang Luo and Yan Guo contributed equally to this work. Xuliang Luo, Yan Guo, Zi Mei, Haobo Zhou, Ping Qiu: designed the experiments. Xuliang Luo, Yan Guo and Zi Mei: Conceptualization, Methodology, Investigation, Writing-original draft, Writing-review. Haobo Zhou, Yan Chen and Haoxing Wang: sample collection. All authors contributed and approved the manuscript. Yanzhang Gong: Conceptualization, Project administration, Writing-review, Funding acquisition. All authors have read and agreed to the published version of the manuscript.

Funding

This work was supported by Genetics of Heterosis in Reproductive Traits in Characteristic Laying Hens (Project No. 2023ZD0405203), Livestock and Poultry Breeding Technology Innovation and the Cultivation and Industrialization of New Varieties (Grant No. 2020ABA016).

Data availability

Proteomics data was deposited into iProX under accession numbers PXD055979.

Declarations

Ethics approval and consent to participate

All animal experiments were carried out following standard procedures and approved by the Ethics Committee of Huazhong Agricultural University, China (ID Number: HZAUCH-2020-0020).

Consent for publication

Not applicable.

Competing interests

The authors declare no competing interests.

Received: 1 January 2025 Accepted: 18 March 2025

Published online: 28 March 2025

References

1. Sabzian-Melei R, Zare-Shahneh A, Zhandi M, Yousefi AR, Rafieian-Naeini HR. Effects of dietary supplementation of different sources and levels of selenium on the semen quality and reproductive performance in aged broiler breeder roosters. *Poult Sci*. 2022;101(10): 101908.
2. Liang W, He Y, Zhu T, Zhang B, Liu S, Guo H, Liu P, Liu H, Li D, Kang X, et al. Dietary restriction promote sperm remodeling in aged roosters based on transcriptome analysis. *BMC Genomics*. 2024;25(1):680.
3. Ali EA, Zhandi M, Towhidi A, Zaghari M, Ansari M, Najafi M, Deldar H. Letrozole, an aromatase inhibitor, reduces post-peak age-related regression of rooster reproductive performance. *Anim Reprod Sci*. 2017;183:110–7.
4. Safari Asl R, Shariatmadari F, Sharafi M, Karimi Torshizi MA, Shahverdi A. Improvements in semen quality, sperm fatty acids, and reproductive performance in aged Ross breeder roosters fed a diet supplemented with a moderate ratio of n-3: n-6 fatty acids. *Poult Sci*. 2018;97(11):4113–21.
5. Simpson ER, Mahendroo MS, Means GD. Aromatase cytochrome P450, the enzyme responsible for estrogen biosynthesis. *Endocr Rev*. 1994;15:342–55.
6. Simkins JW, Joseph AE, Bonier F, Benowitz-Fredericks ZM. Prenatal aromatase inhibition alters postnatal immunity in domestic chickens (*Gallus gallus*). *Gen Comp Endocrinol*. 2020;294: 113497.
7. Singhanian P, Dash D, Dhar A, Biswas P, Gargari P, Bhattacharjee R, Chowdhury S, Datta D, Banerjee E. Aromatase deficiency in a tall man: case report of two novel mutations and review of literature. *Bone Reports*. 2022;17: 101642.
8. Weil S, Rozenboim I, Degen AA, Dawson A, Friedländer M, Rosenstrauch A. Fertility decline in aging roosters is related to increased testicular and plasma levels of estradiol. *Gen Comp Endocrinol*. 1999;115:23–8.
9. Aitken RJ. Impact of oxidative stress on male and female germ cells: implications for fertility. *Reproduction*. 2020;159:R189–201.
10. Pardyak L, Kaminska A, Brzoskwinia M, Hejmej A, Kotula-Balak M, Jankowski J, Cierieszko A, Bilinska B. Differences in aromatase expression and steroid hormone concentrations in the reproductive tissues of male domestic turkeys (*Meleagris gallopavo*) with white and yellow semen. *Br Poult Sci*. 2018;59(5):591–603.
11. Adeldust H, Farzinpour A, Farshad A, Rostamzadeh J, Lopez-Bejar M. Increased sperm cell production in ageing roosters by an oral treatment with an aromatase inhibitor and a natural herbal extract designed for improving fertility. *Reprod Domest Anim*. 2017;52(S4):58–60.
12. Bazary M, Sharafi M, Shahverdi A. Changes in seminal parameters and hormonal profile with use of aromatase inhibitor in management of aging broiler breeder roosters. *Poult Sci*. 2019;98(11):6100–7.
13. Gupta D, Zickler AM, El Andaloussi S. Dosing extracellular vesicles. *Adv Drug Deliv Rev*. 2021;178: 113961.
14. Van Niel G, Carter DRF, Clayton A, Lambert DW, Raposo G, Vader P. Challenges and directions in studying cell-cell communication by extracellular vesicles. *Nat Rev Mol Cell Biol*. 2022;23(5):369–82.
15. Simon C, Greening DW, Bolumar D, Balaguer N, Salamonsen LA, Vilella F. Extracellular vesicles in human reproduction in health and disease. *Endocr Rev*. 2018;39(3):292–332.

16. Luo X, Guo Y, Huang Y, Cheng M, Wu X, Gong Y. Characterization and proteomics of chicken seminal plasma extracellular vesicles. *Reprod Domest Anim.* 2022;57(1):98–110.
17. Thakur BK, Zhang H, Becker A, Matei I, Huang Y, Costa-Silva B, Zheng Y, Hoshino A, Brazier H, Xiang J, et al. Double-stranded DNA in exosomes: a novel biomarker in cancer detection. *Cell Res.* 2014;24(6):766–9.
18. Yanez-Mo M, Siljander PR, Andreu Z, Zavec AB, Borrás FE, Buzas EI, Buzas K, Casal E, Cappello F, Carvalho J, et al. Biological properties of extracellular vesicles and their physiological functions. *J Extracell Vesicles.* 2015;4:27066.
19. Park KHK, Kang J, Nam TS, Lim JM, Kim HT, Park JK, Kim YG, Chae SW, Kim UH. Ca²⁺ signaling tools acquired from prostasomes are required for progesterone-induced sperm motility. *Sci Signal.* 2011;4(173):ra31.
20. Murdica V, Cermisoni GC, Zarovni N, Salonia A, Viganò P, Vago R. Proteomic analysis reveals the negative modulator of sperm function glycodelin as over-represented in semen exosomes isolated from asthenozoospermic patients. *Hum Reprod.* 2019;34(8):1416–27.
21. Utleg AG, Yi EC, Xie T, Shannon P, White JT, Goodlett DR, Hood L, Lin B. Proteomic analysis of human prostasomes. *Prostate.* 2003;56(2):150–61.
22. Baskaran S, Panner Selvam MK, Agarwal A. Exosomes of male reproduction. *Adv Clin Chem.* 2020;95:149–63.
23. Cordeiro LLH, Vitorino Carvalho A, Grasseau I, Uzbekov R, Blesbois E. First insights on seminal extracellular vesicles in chickens of contrasted fertility. *Reproduction.* 2021;161(5):489–98.
24. Luo X, Huang L, Guo Y, Yang Y, Gong P, Ye S, Wang L, Feng Y. Identification of potential candidate miRNAs related to semen quality in seminal plasma extracellular vesicles and sperms of male duck (*Anas Platyrhynchos*). *Poult Sci.* 2024;103(9): 103928.
25. Orsburn BC. Proteome discoverer-a community enhanced data processing suite for protein informatics. *Proteomes.* 2021;9(1): 15.
26. Codesido S, Hanafi M, Gagnebin Y, González-Ruiz V, Rudaz S, Boccard J. Network principal component analysis: a versatile tool for the investigation of multigroup and multiblock datasets. *Bioinformatics.* 2021;37(9):1297–303.
27. Cao T, Li Q, Huang Y, Li A. plotnineSeqSuite: a python package for visualizing sequence data using ggplot2 style. *BMC Genomics.* 2023;24(1):585.
28. Xie C, Mao X, Huang J, Ding Y, Jianmin Wu, Dong S, Kong L, Gao Ge, Li C-Y, Wei L. KOBAS 2.0: a web server for annotation and identification of enriched pathways and diseases. *Nucleic acids research.* 2011;39:W316–22.
29. Franceschini A, Szklarczyk D, Frankild S, Kuhn M, Simonovic M, Roth A, Lin J, Minguez P, Bork P, von Mering C, et al. STRING v9.1: protein-protein interaction networks, with increased coverage and integration. *Nucleic Acids Res.* 2013;41:D808–815.
30. Shannon P, Markiel A, Ozier O, Baliga NS, Wang JT, Ramage D, Amin N, Schwikowski B, Ideker T. Cytoscape: a software environment for integrated models of biomolecular interaction networks. *Genome Research.* 2003;13(11):2498.
31. Tang B, Xie G, Hu X, Zhang X, Hu S, Hu J, Hu B, Li L, Wang J. A comparative proteomic study of high and low semen quality seminal plasma in drakes. *Poult Sci.* 2022;101(11): 102130.
32. Tesfay HH, Sun Y, Li Y, Shi L, Fan J, Wang P, Zong Y, Ni A, Ma H, Mani AI, et al. Comparative studies of semen quality traits and sperm kinematic parameters in relation to fertility rate between 2 genetic groups of breed lines. *Poult Sci.* 2020;99(11):6139–46.
33. Zirkin BR, Chen H. Regulation of Leydig cell steroidogenic function during aging. *Biol Reprod.* 2000;63:977–81.
34. Qi X, Shang M, Chen C, Chen Y, Hua J, Sheng X, Wang X, Xing K, Ni H, Guo Y. Dietary supplementation with linseed oil improves semen quality, reproductive hormone, gene and protein expression related to testosterone synthesis in aging layer breeder roosters. *Theriogenology.* 2019;131:9–15.
35. Xu X, Sun M, Ye J, Luo D, Su X, Zheng D, Feng L, Gao L, Yu C, Guan Q. The effect of aromatase on the reproductive function of obese males. *Horm Metab Res.* 2017;49(08):572–9.
36. Lambeth LS, Morris KR, Wise TG, Cummins DM, O'Neil TE, Cao Y, Sinclair AH, Doran TJ, Smith CA. Transgenic chickens overexpressing aromatase have high estrogen levels but maintain a predominantly male phenotype. *Endocrinology.* 2016;157(1):83–90.
37. Setiawan R, Priyadarshana C, Miyazaki H, Tajima A, Asano A. Functional difference of ATP-generating pathways in rooster sperm (*Gallus gallus domesticus*). *Anim Reprod Sci.* 2021;233: 106843.
38. Rossato M, La Sala GB, Balasini M, Taricco F, Galeazzi C, Ferlin A, Foresta C. Sperm treatment with extracellular ATP increases fertilization rates in in-vitro fertilization for male factor infertility. *Hum Reprod.* 1999;14:694–7.
39. Rodríguez-Miranda E, Buffone MG, Edwards SE, Ord TS, Lin K, Sammel MD, Gerton GL, Moss SB, Williams CJ. Extracellular adenosine 5'-triphosphate alters motility and improves the fertilizing capability of mouse sperm1. *Biol Reprod.* 2008;79(1):164–71.
40. Yi Y-J, Park C-S, Kim E-S, Song E-S, Jeong J-H, Sutovsky P. Sperm-surface ATP in boar spermatozoa is required for fertilization: relevance to sperm proteasomal function. *Systems Biology in Reproductive Medicine.* 2009;55(2–3):85–96.
41. Ford WCL. Glycolysis and sperm motility: does a spoonful of sugar help the flagellum go round? *Hum Reprod Update.* 2006;12(3):269–74.
42. Storey BT. Mammalian sperm metabolism: oxygen and sugar, friend and foe. *Int J Dev Biol.* 2008;52(5–6):427–37.
43. Jeulin C, Soufir JC. Reversible intracellular ATP changes in intact rat spermatozoa and effects on flagellar sperm movement. *Cell Motil Cytoskeleton.* 1992;21:210–22.
44. Bennison C, Hemmings N, Brookes L, Slate J, Birkhead T. Sperm morphology, adenosine triphosphate (ATP) concentration and swimming velocity: unexpected relationships in a passerine bird. *Proceedings of the Royal Society B: Biological Sciences.* 2016;283(1837):20161558.
45. Cao H, Li L, Liu S, Wang Y, Liu X, Yang F, Dong W. The multifaceted role of extracellular ATP in sperm function: from spermatogenesis to fertilization. *Theriogenology.* 2024;214:98–106.
46. Gardella S, Andrei C, Ferrera D, Lotti LV, Torrisi MR, Bianchi ME, Rubartelli A. The nuclear protein HMGB1 is secreted by monocytes via a non-classical, vesicle-mediated secretory pathway. *EMBO Rep.* 2002;3:995–1001.
47. Ronquist KG, Sanchez C, Dubois L, Chioureas D, Fonseca P, Larsson A, Ullén A, Yachnin J, Ronquist G, Panaretakis T. Energy-requiring uptake of prostasomes and PC3 cell-derived exosomes into non-malignant and malignant cells. *Journal of Extracellular Vesicles.* 2016;5(1):29877.
48. Chamberlain KA, Huang N, Xie Y, LiCausi F, Li S, Li Y, Sheng ZH. Oligodendrocytes enhance axonal energy metabolism by deacetylation of mitochondrial proteins through transcellular delivery of SIRT2. *Neuron.* 2021;109(21):3456–3472.e3458.
49. Xia L, Zhang C, Lv N, Liang Z, Ma T, Cheng H, Xia Y, Shi L. AdMSC-derived exosomes alleviate acute lung injury via transferring mitochondrial component to improve homeostasis of alveolar macrophages. *Theranostics.* 2022;12(6):2928–47.
50. Kumar D, Tiwari M, Goel P, Singh MK, Selokar NL, Palta P. Comparative transcriptome profile of embryos at different developmental stages derived from somatic cell nuclear transfer (SCNT) and in-vitro fertilization (IVF) in riverine buffalo (*Bubalus bubalis*). *Veterinary Research Communications.* 2024;48(4):2457–75.
51. Tiwari M, Rawat N, Sharma A, Bhardwaj P, Roshan M, Nagoorvali D, Singh MK, Chauhan MS. Methylation status of imprinted gene IGF2/H19 DMR3 region in Goat (*Capra hircus*) blastocysts produced through parthenogenesis and in vitro fertilization. *Small Ruminant Research.* 2022;216(0):106796–106796.
52. Nawaz S, Hussain S, Bilal M, Syed N, Liaqat K, Ullah I, Akil AAS, Fakhro KA, Ahmad W. A variant in sperm-specific glycolytic enzyme enolase 4 (ENO4) causes human male infertility. *J Gene Med.* 2023;26(1): e3583.
53. Sai Kiran BVS, Srinivasa Prasad CH, Naik BR, Aswani Kumar K, Lavanya S, Nikhil Kumar T, Hyder I. Effect of cryopreservation and capacitation on expression patterns of ATP synthesis associated genes in bubaline spermatozoa. *J Therm Biol.* 2023;117: 103704.
54. Jeanson L, Thomas L, Copin B, Coste A, Sermet-Gaudelus I, Dastot-Le Moal F, Duquesnoy P, Montantin G, Collot N, Tissier S, et al. Mutations in GAS8, a gene encoding a nexin-dynein regulatory complex subunit, cause primary ciliary dyskinesia with axonemal disorganization. *Hum Mutat.* 2016;37(8):776–85.
55. Karachitos A, Kmita H. Voltage-dependent anion channel isoform 3 as a potential male contraceptive drug target. *Future Med Chem.* 2019;11(8):857–67.
56. Mise S, Matsumoto A, Shimada K, Hosaka T, Takahashi M, Ichihara K, Shimizu H, Shiraiishi C, Saito D, Suyama M, et al. Kastor and Polluks

- polypeptides encoded by a single gene locus cooperatively regulate VDAC and spermatogenesis. *Nat Commun.* 2022;13(1):1071.
57. Li C, Yu R, Liu H, Qiao J, Zhang F, Mu S, Guo M, Zhang H, Li Y, Kang X. Sperm acrosomal released proteome reveals MDH and VDAC3 from mitochondria are involved in acrosome formation during spermatogenesis in *Eriocheir sinensis*. *Gene.* 2023;887: 147784.
 58. Pan L, Liu Q, Li J, Wu W, Wang X, Zhao D, Ma J. Association of the VDAC3 gene polymorphism with sperm count in Han-Chinese population with idiopathic male infertility. *Oncotarget.* 2017;8:45242–8.
 59. Woodhouse RM, Frolows N, Wang G, Hawdon A, Wong EHK, Dansereau LC, Su Y, Adair LD, New EJ, Philp AM, et al. Mitochondrial succinate dehydrogenase function is essential for sperm motility and male fertility. *iScience.* 2022;25(12):105573.
 60. Jin S, Hu Y, Fu H, Jiang S, Xiong Y, Qiao H, Zhang W, Gong Y, Wu Y. Identification and characterization of the succinate dehydrogenase complex iron sulfur subunit B gene in the Oriental River Prawn, *Macrobrachium nipponense*. *Frontiers in Genetics.* 2021;12:698318.
 61. Gao Z, Zhang W, Jiang S, Yuan H, Cai P, Jin S, Fu H. Identification of male sex-related genes regulated by SDHB in *Macrobrachium nipponense* based on transcriptome analysis after an RNAi knockdown. *Int J Mol Sci.* 2023;24(17): 13176.
 62. Ryu D-Y, Rahman M, Pang M-G. Determination of highly sensitive biological cell model systems to screen BPA-Related Health Hazards Using Pathway Studio. *Int J Mol Sci.* 2017;18(9): 1909.
 63. Huang S, Wang J, Cui Y. 2,2',4,4'-tetrabromodiphenyl ether injures cell viability and mitochondrial function of mouse spermatocytes by decreasing mitochondrial proteins Atp5b and Uqcrc1. *Environ Toxicol Pharmacol.* 2016;46:301–10.
 64. Tiwari M, Gujar G, Shashank CG, Sriranga KR, Singh RK, Singh N. Omics strategies for unveiling male fertility-related biomarkers in livestock: a review. *Gene Reports.* 2024;35(0):101928–101928.
 65. Huang W, Cao Z, Zhang J, Ji Q, Li Y. Aflatoxin B1 promotes autophagy associated with oxidative stress-related PI3K/AKT/mTOR signaling pathway in mice testis. *Environ Pollut.* 2019;255(Pt 2): 113317.
 66. Ma F, Zhou Z, Li N, Zheng L, Wu C, Niu B, Tang F, He X, Li G, Hua J. Lin28a promotes self-renewal and proliferation of dairy goat spermatogonial stem cells (SSCs) through regulation of mTOR and PI3K/AKT. *Sci Rep.* 2016;6: 38805.
 67. Hu C, Zuo Q, Jin K, Zhao Z, Wu Y, Gao J, Wang C, Wang Y, Zhan W, Zhou J, et al. Retinoic acid promotes formation of chicken (*Gallus gallus*) spermatogonial stem cells by regulating the ECM-receptor interaction signaling pathway. *Gene.* 2022;820: 146227.

Publisher's Note

Springer Nature remains neutral with regard to jurisdictional claims in published maps and institutional affiliations.